

## RESISTIVE PRESSURE SENSORS INTEGRATED WITH A CORIOLIS MASS FLOW SENSOR

*D. Alveringh<sup>1</sup>, T.V.P. Schut<sup>1</sup>, R.J. Wiegerink<sup>1</sup>, W. Sparreboom<sup>2</sup>, and J.C. Lötters<sup>1,2</sup>*

<sup>1</sup> MESA+ Institute for Nanotechnology, University of Twente, Enschede, The Netherlands

<sup>2</sup> Bronkhorst High-Tech BV, Ruurlo, The Netherlands

### ABSTRACT

We report on a novel resistive pressure sensor that is completely integrated with a Coriolis mass flow sensor on one chip, without the need for extra fabrication steps or different materials. Two pressure sensors are placed in-line with the Coriolis sensor without requiring any changes to the fluid path. This enables the measurement over the pressure drop of the Coriolis mass flow sensor and  $\Delta P$  flow sensing. By combining this pressure drop with the output signal of the Coriolis mass flow sensor, real-time viscosity characterization is also possible. Since the pressure sensor consists of a Wheatstone bridge, no complex interfacing electronics are needed. The first characterization of the sensor shows a linear sensitivity of  $4\ \mu\text{V bar}^{-1}$  for a pressure range from 0 bar to 1 bar.

### KEYWORDS

Pressure sensor, Coriolis mass flow sensor, multi parameter system, viscosity sensor, density sensor, surface channel technology.

### INTRODUCTION

Numerous microfabricated flow sensors and pressure sensors have been developed during the last decades, e.g. thermal flow sensors [1, 2], Coriolis flow sensors [3, 4] and pressure sensors [5, 6]. Usually each sensor has its own unique fabrication process and combining multiple sensors on a single chip is nearly impossible. As a consequence, combining e.g. a pressure and a flow sensor on a single chip to not only measure pressure and flow, but also a fluid parameter like viscosity, is not possible. In [7, 8], we made a first attempt to integrate flow sensors and pressure sensors on a single chip, but in that case the pressure sensor had a capacitive readout with low sensitivity and large drift. Furthermore, multiple capacitive sensors on one chip may introduce crosstalk, and in [7, 8] the sensors were not operated simultaneously.

In this paper, we present a resistive pressure sensor that is integrated with a Coriolis mass flow sensor without any changes in the fabrication process. The resistive structures are more straight forward to interface and hardly influence the capacitive readout of the Coriolis mass flow sensor. Two inline resistive pressure sensors are integrated both upstream and downstream of a Coriolis mass flow sensor, as illustrated in Figure 1. The Coriolis mass flow sensor provides direct mass flow and density information. The pressure sensors provide a measure for the pressure drop over the Coriolis mass flow sensor. Combination

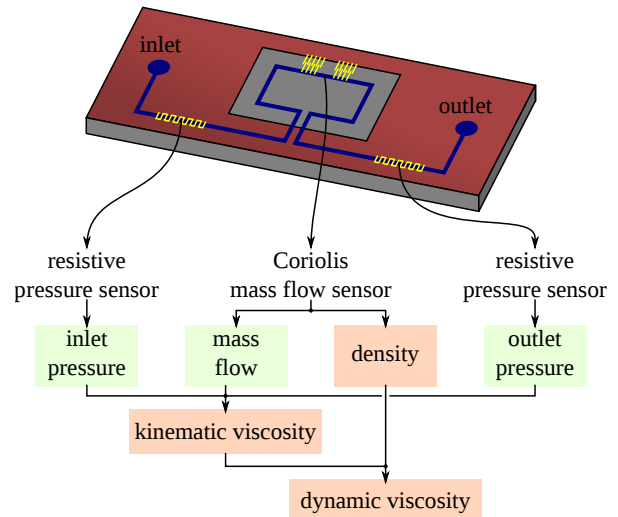


Figure 1: Integration of two resistive pressure sensors with a capacitive Coriolis mass flow sensor on one chip. The multiple sensors allow for the measurement of flow and pressure, and therefore enable the derivation of viscosity.

of the measured variables enables the derivation of the viscosity.

### PRESSURE SENSING

Similar to [7, 8], the pressure sensors are integrated in the supply and exhaust channels of the Coriolis mass flow sensor. The pressure sensors therefore do not introduce extra volumes or larger pressure drop. The channels are semi-circular with a flat ceiling and made of silicon nitride, as indicated in Figure 2. A pressure inside the channel deforms the ceiling. Thin-film gold resistors are deposited on top of the channel. The resistors have a meandering shape to increase sensitivity. They are connected in a Wheatstone bridge as indicated in the figure. Two resistors of the bridge are placed over the center of the channel and will elongate due to the deformation; the other two resistors are placed at the sides and will be compressed.

The membrane of the channel is modeled as a clamped-clamped beam of silicon nitride using a finite element model in COMSOL Multiphysics 4.3 with the dimensions given in Table 1. By integrating the strain on top of the membrane, an approximation of the elongation of the resistors is found. The obtained elongations are also shown in Table 1. The resistance for all four resistors is proportional to the elongation:

$$R_i \propto L_R + \Delta L_{R_i}, \quad (1)$$

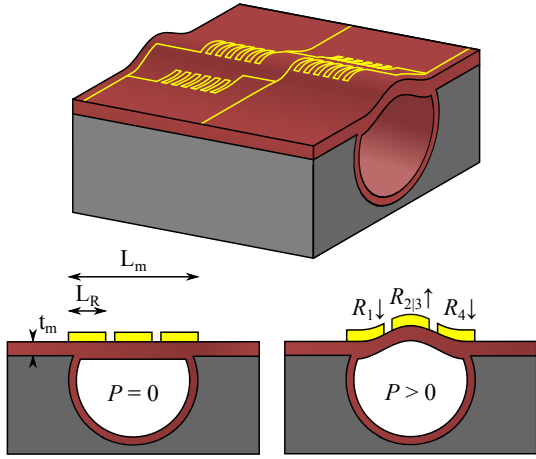


Figure 2: Illustration of the resistive pressure sensor. The non-circularly shaped channel deforms due to pressure and elongates/compresses the thin-film electrodes on the ceiling.

with  $R_i$  resistor  $i$ ,  $L_R$  the length of one resistor segment and  $\Delta L_{R_i}$  the elongation of resistor  $i$ . The output voltage  $V_{out}$  of the Wheatstone bridge is defined as follows:

$$V_{out} = \left( \frac{R_2}{R_1 + R_2} - \frac{R_4}{R_3 + R_4} \right) V_{in}, \quad (2)$$

with  $V_{in}$  the input voltage of the Wheatstone bridge. As explained below, we use an AC voltage with an amplitude of 100 mV. Substitution of the numbers from Table 1 in Equations 1 and 2 results in a theoretical sensitivity of  $4.9 \mu\text{V bar}^{-1}$ .

Table 1: Dimensions and results of the finite element model.

Pressure	$P$	1 bar
Membrane thickness	$t_m$	$1.5 \mu\text{m}$
Membrane width	$L_m$	$42 \mu\text{m}$
Resistor segment length	$L_R$	$14 \mu\text{m}$
$R_1$ elongation	$\Delta L_{R_1}$	$-0.46 \text{ nm}$
$R_2$ elongation	$\Delta L_{R_2}$	$0.92 \text{ nm}$
$R_3$ elongation	$\Delta L_{R_3}$	$0.92 \text{ nm}$
$R_4$ elongation	$\Delta L_{R_4}$	$-0.46 \text{ nm}$

### MULTI PARAMETER SENSING

The capacitive Coriolis mass flow sensor design was presented in [4]. Coriolis mass flow sensors measure the true mass flow and are independent of temperature, pressure and fluidic parameters like density and viscosity. This sensor is actuated at its resonance frequency. The frequency is dependent on the mass of the vibrating channel and therefore dependent on the density of the fluid. An extensive analysis of this sensor is published in [9].

For incompressible Newtonian fluids at low Reynolds numbers, the flow through the Coriolis mass flow sensor will obey the Hagen-Poiseuille law. In our experiments, we have used water and isopropyl alcohol with mass flows under  $15 \text{ g h}^{-1}$ , so that this is the case. Therefore, the dynamic viscosity  $\eta$  is proportional to the ratio of the pressure drop

$\Delta P$  and the volume flow  $Q$ :

$$\eta \propto \frac{\Delta P}{Q} = \frac{\Delta P \rho}{\Phi}. \quad (3)$$

with  $\rho$  the density and  $\Phi$  the mass flow, which are both measured by the Coriolis mass flow sensor. The kinematic viscosity  $\nu$  can be derived directly from mass flow without density information, since  $\nu = \eta/\rho$ .

### DEVICE FABRICATION

Test devices have been designed and fabricated. The fabrication process has been presented before in [10]. A scanning electron microscopy image of the device is shown in Figure 3).

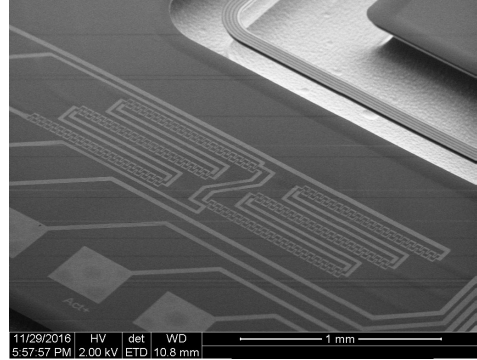


Figure 3: Scanning electron microscopy image of the pressure sensor. In this case, the sensor contains three parallel channels to reduce the pressure drop. This allowed for the integration of three pressure sensors.

### MEASUREMENT SETUP

The chip is mounted and wire bonded on a printed circuit board. The fluid inlet and outlet are located at the bottom of the printed circuit board, as illustrated in Figure 5. The inlet is connected to a vessel containing water or isopropyl alcohol. The pressure in the vessel is controlled using nitrogen gas. The outlet is connected to a mass flow controller. With this setup, two different types of measurements are conducted:

- a pressure sensor calibration at different pressures, but without flow;
- multi parameter measurements using water and isopropyl alcohol at different pressures and mass flows.

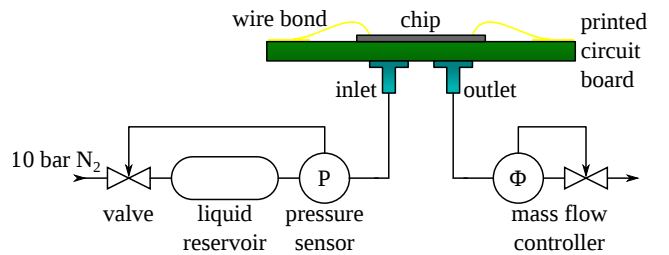


Figure 5: Assembly of the chip with the fluidic measurement setup. At the inlet, the pressure of different liquids can be controlled. The mass flow is controlled at the outlet.

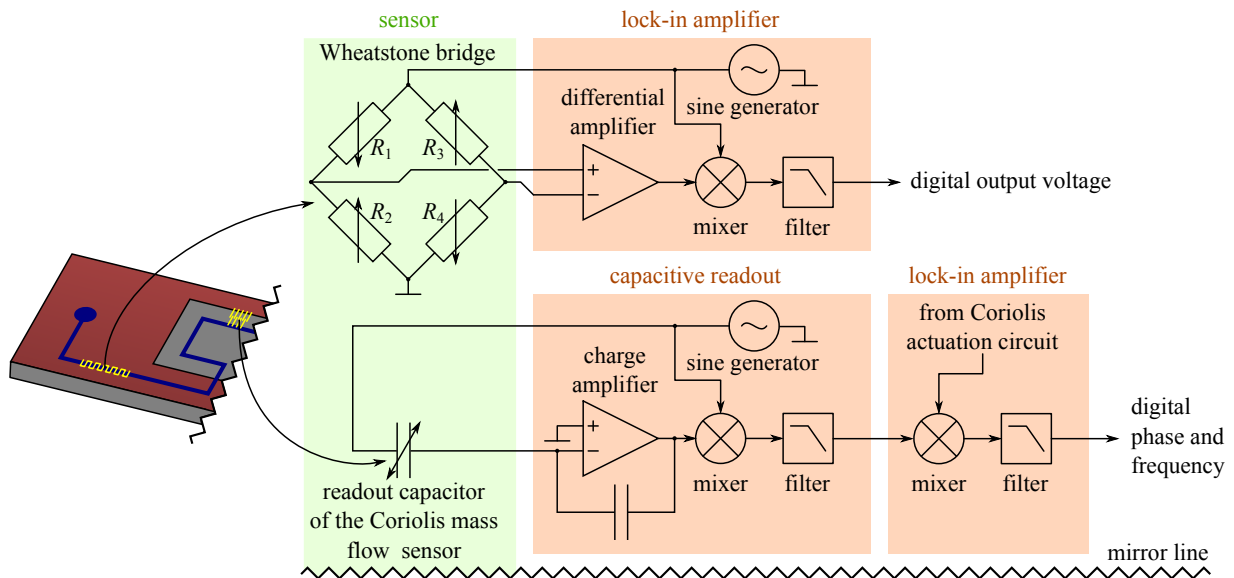


Figure 4: The electronic interfacing of both sensors. A 100 mV signal with a frequency of  $\sim 1$  kHz is fed to the Wheatstone bridge. The signal from the readout terminals is demodulated and filtered by a lock-in amplifier. The Coriolis mass flow sensor is interfaced using custom demodulation electronics and a lock-in amplifier for frequency and phase detection. Only half of the setup is shown.

Figure 4 shows the electronic interfacing of both the pressure sensor and the Coriolis mass flow sensor. The Wheatstone bridges are fed by sine wave with an amplitude of 100 mV and a frequency of  $\sim 1$  kHz. The output terminals are connected to the differential input of a lock-in amplifier. The readout capacitances of the Coriolis mass flow sensor are converted to voltages using charge amplifiers and then demodulated. A lock-in amplifier is synchronized with the actuation frequency and measures the frequency and phase of the two output signals.

For the multiparameter measurements, both pressure sensors and the Coriolis mass flow sensor have been read out simultaneously. Mass flows are varied between  $0 \text{ g h}^{-1}$  and approximately  $12 \text{ g h}^{-1}$  for gauge pressures of 3 bar, 4 bar, 5 bar and 6 bar for both water and isopropyl alcohol. Figure 7 shows the output signal (phase shift) of the Coriolis mass flow sensor against mass flow. It appears that the phase shift is almost only dependent on mass flow and independent of pressure or density.

## CHARACTERIZATION

For the pressure sensor calibration, gauge pressures are applied using a pressure controller from 0 bar to 1 bar in steps of 0.1 bar. The results in Figure 6 show no hysteresis and a linear response with a sensitivity of  $4 \mu\text{V bar}^{-1}$ . Robustness tests show that the sensor can handle at least 10 bar.

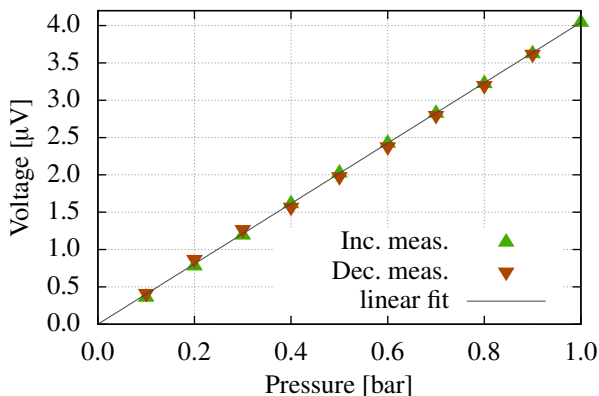


Figure 6: Measurement results for increasing and decreasing gauge pressures ranging from 0 bar to 1 bar. The measurement results are corrected for offset.

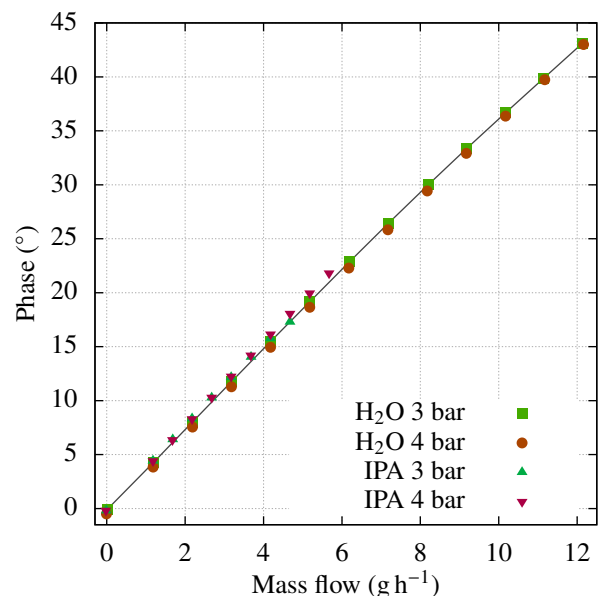


Figure 7: Phase shift as a result of mass flow through the Coriolis mass flow sensor for water and isopropyl alcohol for pressures of 3 bar and 4 bar. The mass flows were varied between  $0 \text{ g h}^{-1}$  and approximately  $12 \text{ g h}^{-1}$ .

Figure 8 shows the resonance frequency of the Coriolis mass flow sensor. The frequency is very dependent on density (128 Hz difference between water with  $1000 \text{ kg m}^{-3}$  and isopropyl alcohol with  $785 \text{ kg m}^{-3}$ ) and slightly dependent on pressure ( $7.2 \text{ Hz bar}^{-1}$ ).

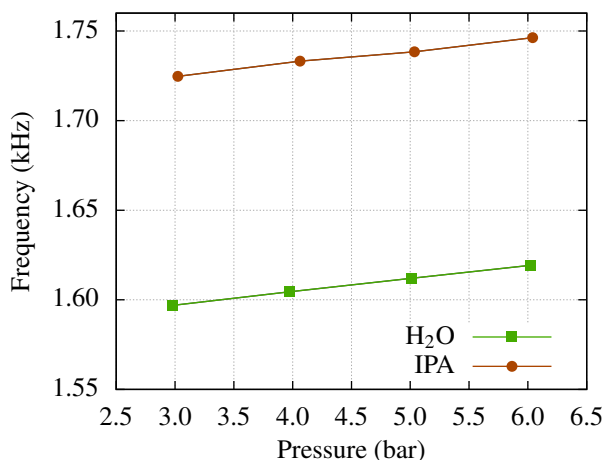


Figure 8: The resonance frequency of the Coriolis mass flow sensor for water and isopropyl alcohol for pressures between 3 bar and 6 bar.

The pressure drop is proportional to the mass flow. The slope appears to be defined by the fluid parameters, since the pressure drop for isopropyl alcohol is three times higher than for water. Using Equation 3 and water as reference, the dynamic viscosity of isopropyl alcohol was measured to be approximately  $2.4 \text{ mPa s}$ .

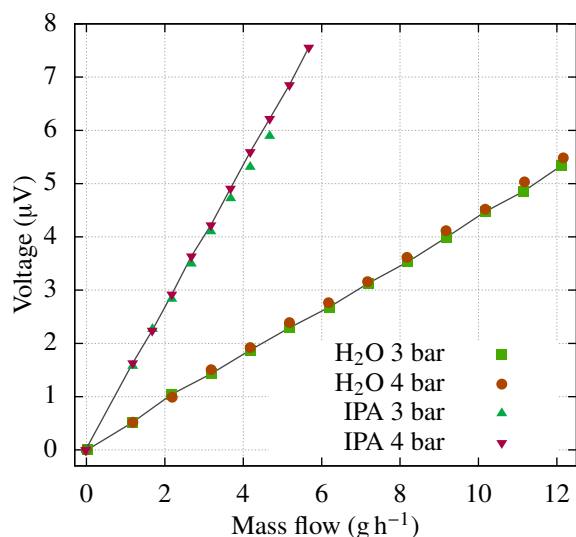


Figure 9: The pressure drop over the Coriolis mass flow sensor for water and isopropyl alcohol for pressures of 3 bar and 4 bar. The mass flows were varied between  $0 \text{ g h}^{-1}$  and approximately  $12 \text{ g h}^{-1}$ .

## CONCLUSION

Two resistive pressure sensors have been integrated with a capacitive Coriolis mass flow sensor on a single chip. Characterization of the pressure sensors shows a

linear response with a sensitivity of  $4 \mu\text{V bar}^{-1}$ . Density and mass flow have been measured by the Coriolis mass flow sensor. The pressure information can be used to measure the viscosity of the fluid. Besides, it could be used to compensate for pressure dependent behavior of the Coriolis mass flow sensor and increase its sensitivity.

Future work will focus on the characterization of the sensor with gases.

## ACKNOWLEDGEMENTS

The authors gratefully acknowledge financial support by the Eurostars Programme through the TYPICAL project (E!8264) and R.G.P. Sanders for technical support.

## REFERENCES

- [1] A. F. P. Van Putten *et al.*, "Integrated silicon anemometer," *Electronics Letters*, vol. 10, no. 21, pp. 425–426, 1974.
- [2] N. T. Nguyen, "Micromachined flow sensors - a review," *Flow measurement and Instrumentation*, vol. 8, no. 1, pp. 7–16, 1997.
- [3] P. Enoksson *et al.*, "A silicon resonant sensor structure for coriolis mass-flow measurements," *Journal of Microelectromechanical Systems*, vol. 6, no. 2, pp. 119–125, 1997.
- [4] J. Haneveld *et al.*, "Modeling, design, fabrication and characterization of a micro coriolis mass flow sensor," *Journal of Micromechanics and Microengineering*, vol. 20, no. 12, p. 125001, 2010.
- [5] W. P. Eaton *et al.*, "Micromachined pressure sensors: review and recent developments," *Smart Materials and Structures*, vol. 6, no. 5, p. 530, 1997.
- [6] Y. Zhang *et al.*, "A high-sensitive ultra-thin MEMS capacitive pressure sensor," in *The 16th International Solid-State Sensors, Actuators and Microsystems Conference (TRANSDUCERS)*. IEEE, 2011, pp. 112–115.
- [7] J. C. Lötters *et al.*, "Integrated multi-parameter flow measurement system," in *The IEEE 27th International Conference on Micro Electro Mechanical Systems (MEMS)*. IEEE, 2014, pp. 975–978.
- [8] D. Alveringh *et al.*, "Inline pressure sensing mechanisms enabling scalable range and sensitivity," in *The 18th International Conference on Solid-State Sensors, Actuators and Microsystems (TRANSDUCERS)*. IEEE, 2015, pp. 1187–1190.
- [9] J. Groenesteijn, *Microfluidic platform for Coriolis-based sensor and actuator systems*. Enschede: Twente University Press, January 2016.
- [10] M. Dijkstra *et al.*, "A versatile surface channel concept for microfluidic applications," *Journal of Micromechanics and Microengineering*, vol. 17, no. 10, p. 1971, 2007.

## CONTACT

Dennis Alveringh, d.alveringh@utwente.nl.